

# Testing of a Clinical Tremor Analysis System

Hailey Cunningham<sup>1</sup>, Justin Lee<sup>1</sup>, Soohyun Myung<sup>1</sup>

<sup>1</sup>Department of Electrical and Computer Engineering  
The George Washington University  
Washington DC, United States of America

**Abstract**— Finding a cheap and efficient way to detect and characterize the extent of physiological tremors can benefit both sufferers of neurological conditions and physical therapy patients. This paper presents a novel way for tremor detection and characterization using just a webcam and a strap that holds two LEDs used in conjunction with a traditional sensor setup. This paper seeks to describe the validity of the novel system through two means of testing. The first testing method consists of using a cam driving a lever arm up and down at a known frequency. The second involves using an electric stimulator to send a train of pulses at a known frequency into the arm of a human test subject in order to induce finger twitches. The results demonstrate an ability to accurately detect the known frequency in both the novel optical system and the traditional system between 3 and 10 Hz. However, limitations to the testing methods prevented analysis of the full range frequencies that physiological tremors cover. Nevertheless, linear regression analyses indicate the strong correlation between known and detected frequency data from both subsystems. This demonstrates the validity of the new optical system in detecting and analyzing tremors, creating a cheap method that has implications for telemedicine.

**Keywords**—tremor, testing, optical, sensor, comparisons

## I. INTRODUCTION

Tremors are often symptoms that arise from underlying neurological and physiological conditions that affect many individuals. Tremors are defined by the oscillation of a limb through prolonged cycles of muscle contraction and relaxation. Whether induced in a healthy individual by means of stroke, traumatic brain injury or muscle fatigue or existent as symptoms of neurological conditions such as Parkinson's disease and cerebral palsy, the presence of tremors impede physiological function and the carrying out of daily activities. Depending on the severity of the tremor, the suffering individual will experience changes in lifestyle to better overcome the inhibitions. The difficulty to perform the daily tasks of life, such as those requiring fine motor skills such as eating and writing, can bring physical, emotional and social insecurities. Therefore, proper study of the tremors in the clinical setting is imperative to better understand its biomechanics, improve diagnosis and help develop appropriate therapies that will treat or reduce the severity of the tremor.

Current methods of characterizing tremors often use accelerometers. The Clinical Tremor Analysis System builds on this, using a tri-axial accelerometer and tri-axial angular rate sensor in addition to a novel optical method using LEDs and a webcam to detect tremor. These two tremor detecting methods are connected via the data analysis subsystem to get

meaningful clinical data. The system also seeks to determine the validity of the novel optical subsystem. If it proves to be as effective in sensing tremors as the sensor subsystem, the optical subsystem could revolutionize tremor detection and characterization both in economic cost and in telemedicine.

## II. THEORY OF OPERATION

The Clinical Tremor Analysis System records motion in two ways, an optical subsystem and a sensor subsystem, with a data analysis subsystem that unifies the two. The sensor subsystem consists of a tri-axial accelerometer and a tri-axial angular rate sensor. These two sensors record accelerations and rates of rotation in the x, y and z axes. The two sensors of the sensor subsystem are controlled with a microcontroller that adjusts settings, receives raw data and converts it to usable data. The microcontroller then sends that data off to the data analysis system.

The optical subsystem consists of two LEDs attached to the palm of the hand or the finger and a webcam. The LED circuit attached to the limb undergoing tremor moves with the tremor and the webcam captures the motion of the LEDs. The webcam feed is then sent off to the data analysis subsystem.

The data analysis subsystem takes the data from the sensor and optical subsystem and analyzes it for frequency information. The webcam feed is analyzed to find and track the center of and calculate the angle between the two LEDs. It then takes the Fast Fourier Transforms (FFTs) of the optical position and angular data and the sensor. Finally, the FFTs are analyzed for shared peaks.

## III. TESTING METHODS

Two main methods were employed when testing this system; measuring a known frequency created by a motor and measuring induced tremors using a stimulating electrode. The first method was used to validate the readings from the sensors and the optical subsystem against known data, while the second was used to simulate readings that might occur in a clinical setting and to test the ability of the system to read them.

### A. Method 1: Testing Rig

For the first method a testing rig was built to create the periodic motion. The rig consists of a thin board attached to the base via a hinge. Underneath the thin board there is a cam on a shaft with a small gear at the other end. The small gear meshes with a larger gear attached to the stepper motor to increase the

speed of rotation of the cam. The stepper motor is controlled through a driver and microcontroller attached to a computer. Underneath the cam is a secondary speed measuring system consisting of a switch which completes a circuit when pressed, the output of which can be seen in an oscilloscope to measure the actual speed of the cam. This setup can be seen in Fig. 1.

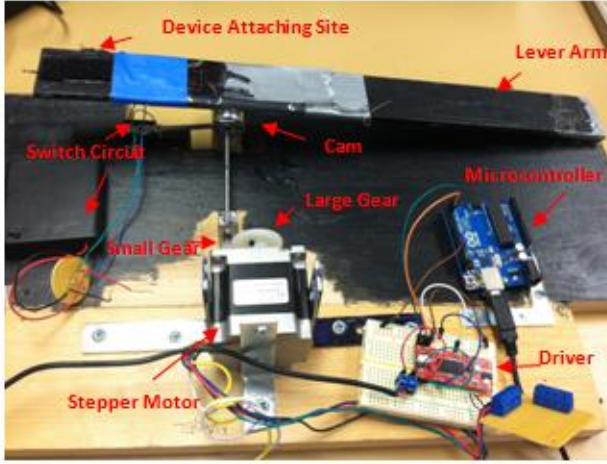


Fig 1. Testing rig (labeled)

In testing with this system the first test was to confirm that the speed that the microcontroller was setting the motor to run at was the same as the actual speed of the motor. This was done by comparing the speed input into the program to the speed measured by the switch underneath the cam at various speeds. The results of the verification can be seen in Fig. 2. The validation demonstrates that the calculated and actual speeds of the motor were very similar with an  $R^2$  value of 0.9989.

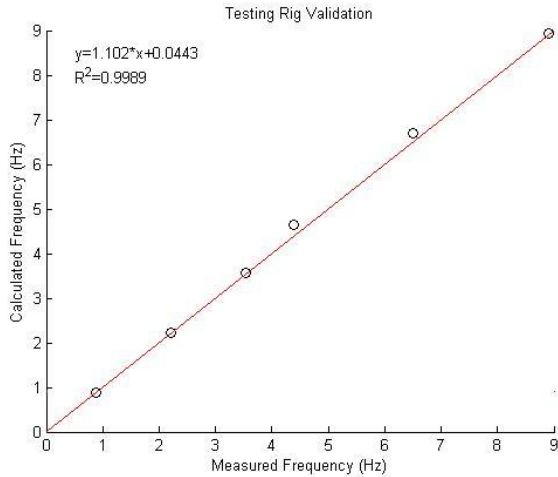


Fig 2. Testing Rig Validation

Once the verification of the testing rig had been completed, the two tremor measuring subsystems were tested on the system. Each system in turn was attached to the board at the location indicated in Fig. 1. Then the subsystem was subjected to a range of frequencies. For each frequency, the FFT of that measurement was saved through the data analysis system and the peaks were found. The peak pertaining to the frequency of

the motion was compared to the actual speed of the cam's rotation. For the sensor subsystem, data was collected from 1-11 Hz. For the optical subsystem data was collected from 1-10 Hz due to issues with the changing frame rate of the webcam from changing frame causing discrepancies in the data.

#### B. Method 2: Stimulator Test

The second method of testing was to induce tremors in a subject and to measure those tremors with each of the tremor detecting subsystems. To induce tremors a BIOPAC Human Stimulator Probe was used to stimulate muscles in the forearm to induce a finger to twitch. The sensor subsystem and the optical subsystem were positioned in such a way that the motion of the finger twitch could be recorded. By applying stimuli at a certain frequency it is possible to make the finger twitch faster or slower. Whether the frequency of stimulation is the same as the frequency of the finger twitch is not known for sure, as such it can only be approximated that the finger is moving at the same frequency as the stimulation.

Testing using the electrode was done for each subsystem by sweeping the frequency of stimulation from 1-11 Hz. Results from higher frequencies were unable to be obtained due to the fact that attempting to stimulate a muscle with shorter times between each stimulation requires a larger voltage stimulation until it becomes impossible. At higher frequencies than 11 Hz the required stimulation for a twitch caused pain in the subject. In addition the twitch was unable to be sustained for long enough to get distinct frequencies due to fatigue. For these reasons, the data for human testing using the electrode was only used up to 11 Hz. This process was repeated for both the sensor and the optical subsystems

### IV. TESTING RESULTS

The following table summarized the original requirements and specifications of the system as a whole and the results of the current system.

TABLE I. REQUIREMENTS AND SPECIFICATIONS

Functional Requirements	Specifications	Results
(1) System must be able to capture the motion of a limb	<ul style="list-style-type: none"> <li>System must be able to capture tremors with frequency from 0.5 Hz to 15 Hz</li> </ul>	<ul style="list-style-type: none"> <li>System can capture motion between less than 0.5 Hz and 12 Hz</li> </ul>
(2) System will capture motion of a limb with a three axis accelerometer	<ul style="list-style-type: none"> <li>Accelerometer will detect acceleration in the range of <math>\pm 2g</math></li> <li>Accelerometer sensitivity 240 LSB/g</li> </ul>	<ul style="list-style-type: none"> <li>This is met by the specifications of the sensor bought<sup>a</sup></li> </ul>
(3) System will capture motion of a limb with a three axis angular rate sensor	<ul style="list-style-type: none"> <li>Angular rate sensor will be able to detect a rate of rotation of up to 500 degrees/s</li> <li>Angular rate sensor sensitivity should be at least 60 LSB/degree/s</li> </ul>	<ul style="list-style-type: none"> <li>This is met by the specifications of the sensor bought<sup>b</sup></li> </ul>

(4) System must be able to capture and store data for the subsystem	<ul style="list-style-type: none"> <li>Frequency of data capture will be at least 30 Hz for the accelerometer and the angular rate sensor</li> <li>Frequency of data capture will be at least 30 fps</li> </ul>	<ul style="list-style-type: none"> <li>The sensor subsystem captures at 26 Hz</li> <li>The optical subsystem captures at 29-30 fps</li> </ul>
(5) System will capture motion of a limb with an optical system consisting of an LED and capture device	<ul style="list-style-type: none"> <li>Will detect displacement across the maximum range of pixels in both the width and height of the image</li> <li>Will detect a change in position of 1.0 mm</li> </ul>	<ul style="list-style-type: none"> <li>The data analysis system can detect the LEDs across the whole width of the image</li> <li>Small position change detection is controlled by distance from webcam</li> </ul>
(6) System must be able to analyze measured limb motions from the three subsystems	<ul style="list-style-type: none"> <li>Fourier transforms</li> <li>Determine intensity of center of LEDs based on video feed to within a half a pixel</li> </ul>	<ul style="list-style-type: none"> <li>System takes Fourier transforms of all data</li> <li>System determines center of LEDs through LabVIEW</li> </ul>
(7) System must display data in a way determined by the user	<ul style="list-style-type: none"> <li>System must display the user's choice of the following data over time and its corresponding Fourier transform <ul style="list-style-type: none"> <li>Accelerometer data: <ul style="list-style-type: none"> <li>Accelerations (<math>\ddot{x}, \ddot{y}, \ddot{z}</math>)</li> <li>Velocities (<math>\dot{x}, \dot{y}, \dot{z}</math>)</li> <li>Positions (<math>x, y, z</math>)</li> </ul> </li> <li>Angular rate sensor data <ul style="list-style-type: none"> <li>Rate of angle change (<math>\dot{\theta}, \dot{\phi}, \dot{\rho}</math>)</li> <li>Angles (<math>\theta, \phi, \rho</math>)</li> </ul> </li> <li>Optical data <ul style="list-style-type: none"> <li>Position in x</li> <li>Position in y</li> </ul> </li> </ul> </li> <li>System will have options to display graphs comparing: <ul style="list-style-type: none"> <li>Positional data from accelerometer converted to angles with angles from angular rate sensor (all three axis)</li> <li>Position data in x and y from optical system and position data in x and y from accelerometer</li> </ul> </li> <li>System will display the mapping of the optical system <ul style="list-style-type: none"> <li>In either Cartesian coordinates (x, y) or polar coordinates (r, <math>\theta</math>) about the origin (center point)</li> </ul> </li> </ul>	<ul style="list-style-type: none"> <li>The display shows accelerations and rate of angle changes from the sensor subsystem and positions and angles from the optical subsystem</li> <li>Integrated data is not displayed due to drift.</li> <li>The system has a save feature and saved data display feature</li> <li>Comparisons are done through peak detection of the FFTs of each axis of each sensor and optical element</li> </ul>
(8) System must compare values obtained from the three subsystems	<ul style="list-style-type: none"> <li>System will compare angles from the angular rate sensor in all three axes with derived angles from the accelerometer. The comparison should result in a 1:1 slope</li> <li>System will compare the positional data in the x and y axis from the accelerometer and the positional data from the</li> </ul>	<ul style="list-style-type: none"> <li>Comparisons are done using peak detection of FFTs of the pertinent data</li> </ul>

	optical system. The comparison should result in a 1:1 slope	
Non-Functional Requirements	Specifications	Results
(9) The system must be small and light enough to not interfere with limb tremors	<ul style="list-style-type: none"> <li>Under 75 grams</li> <li>Housing for accelerometer and angular rate sensor should be under 3 cm x 3 cm x 1 cm</li> <li>Housing for LED in optical subsystem should be under 2 cm x 2 cm x 1 cm</li> </ul>	<ul style="list-style-type: none"> <li>Weight of the wristband is 23.14 g</li> <li>Weight of the ring is 6.34 g</li> <li>Housing for sensor subsystem is 4.8 cm x 3 cm x 1.5 cm</li> <li>Optical subsystem is not in a housing</li> </ul>
(10) The system must be capable of being attached to various parts of the body	<ul style="list-style-type: none"> <li>Strap for use on wrist will fit wrists from 12-28 cm in circumference</li> </ul>	<ul style="list-style-type: none"> <li>The wrist strap can fit wrists from 10 - 21 cm</li> </ul>
(11) The system must be wearable by the user without assistance from another	<ul style="list-style-type: none"> <li>Strap will use Velcro to attach</li> </ul>	<ul style="list-style-type: none"> <li>The ring and wristband attach via Velcro</li> </ul>

<sup>a</sup> See reference [1] for data sheet

<sup>b</sup> See reference [2] for data sheet

Many of the differences between the original design specifications and the current specifications are due to changes in design. For (9) the decision was made to have no housing for the optical subsystem and the size of the housing of the sensor subsystem was limited by the size of the sensor breakout board. For (10) the wrist strap is mostly used on the hand so the dimensions are slightly different. The information needed for display in (7) has changed over time as it was considered what is important to display. Finally, the style of comparisons has changed from directly comparing data to peak detection in the FFTs. The changes in specifications pertaining to frequency will be discussed in the following subsections.

#### A. Testing Rig Experiments

Both the sensor and optical subsystems were hooked up to each testing situation separately. Data was taken for each subsystem in turn. A single test iteration consisted of adjusting the known frequency of either the testing rig or the stimulator to the desired value and recording data for around 5 seconds. The recorded data is then converted to frequency domain where local maximums indicate characteristic frequency components that make up the time-domain waveform.

The testing rig registered in both angular and positional/accelerometer data as a series of up and down motions that appeared as jagged peaks. Since the motion of the lever arm is very rigid, the recorded data resembles a triangular waveform. While the most prominent frequency, the one driving the system, is generally the frequency with the highest amplitude, other local maxima exist throughout the frequency range. Data gathered from both systems reveal that at fast frequencies, between 10 to 12 Hz, the triangular waveform is distorted. The amplitude between each period changes drastically. Even the period itself is unpredictable.

The researchers have determined that at these frequencies, the cam is generating enough force to create a bounce in the lever arm. The bounce causes the lever arm to remain in the air for a short period of time before landing back onto the cam, creating moments in both the amplitude and the period that are uncontrolled. While this bounce is damped slightly by rubber band, it is still largely present. This is nonexistent for lower frequencies because they cannot generate the force to impart energy to the lever arm in the same way. As a result though, the data for anything past 10 Hz is unreliable. This problem disappears for frequencies below 10 Hz.

For this paper, the detected frequencies that are closest to the input frequencies are plotted against the input in order to determine a linear relationship. The linearity gives validity to both the sensor and optical subsystems. The sensor subsystem on the testing rig gives the relationship shown in Fig. 3.

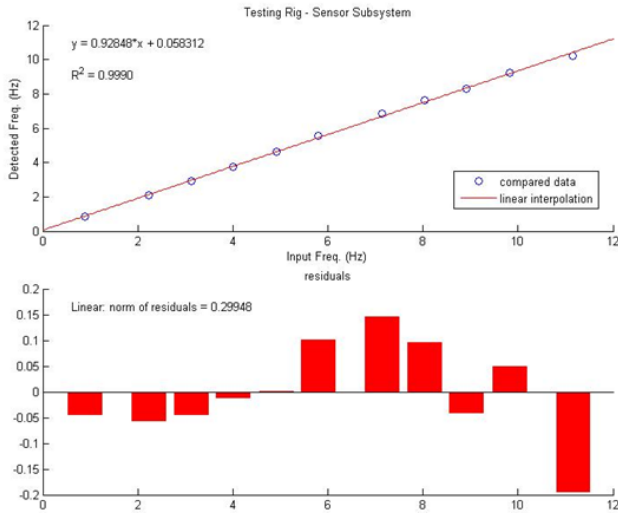


Fig 3. Testing Rig – Sensor Subsystem

The data is plotted on MATLAB. A least squares fitting algorithm found in the basic fitting package is used to determine the linear regression line. Corresponding residuals of each data point is displayed below the linear regression plot for comparison. Least squares fitting found the slope of the sensor subsystem to be  $b=0.92828$ , a slope that is close to 1. The goodness-of-fit is evidenced by an  $R^2$  value of 0.9990. The size of the residuals increases as higher frequencies are tested, indicating that the system gets less accurate as the cam rotates at higher frequencies. This makes sense in light of the lever arm bounce that was described earlier. Faster cam rotations convey more force to the lever arm. This in turn separates the actual frequency from the expected value, creating high residuals. Trying to test for 11 Hz, for example, fell far short of its actual value, as indicated by a residual value of -0.2. This indicates a limited range on which the system can be tested on the testing rig.

The optical subsystem was tested in the same method as the sensor subsystem. The comparison relationship is demonstrated in Fig. 4.

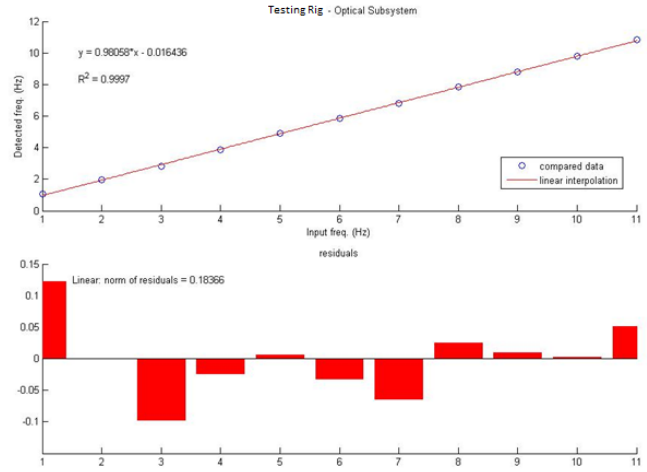


Fig 4. Testing Rig – Optical Subsystem

Least squares fitting on the optical subsystem corresponds to a slope of  $b=0.98058$  and an  $R^2$  value of 0.9997. This subsystem has a more linear correlation than the sensor subsystem, but becomes increasingly more difficult to use on higher frequencies. The residuals are much smaller than the ones for the sensor subsystem. An anomaly seems to be the high value of the residual for the 1 Hz frequency. However, 1 Hz moves the cam at such a slow place that the change in LED position barely registers on the webcam. The detected frequency is small as a result. In order to capture motion in higher frequencies, the camera needs a much faster frame rate in order to fulfill Nyquist criteria. Right now, 12 Hz seems to be the limit for using the optical subsystem to capture data from the testing rig. In addition, frame rate changes produce stutters in the data collection that appear as small spikes in the positional and angular data. The spikes introduce new frequency components in the FFT. Future implementations will require the use of a camera that captures at a constant frame rate.

## B. Stimulator Experiments

Twitches that result from stimulator shocks registered as nearly triangular pulses, with the ramp up portion corresponding to a finger curling inwards and the ramp down portion corresponding to a finger relaxing. This motion is detected in the y and z angular rate change and the z acceleration change. The jaggedness of the waveforms created frequency spectra that smeared out across the frequency ranges, most noticeable between 1 and 3 Hz. During this time, the pulse frequencies were slow enough to be indistinguishable from the natural vibrations and accidental movements of the hand or the finger. Unexpected frequencies appeared as a result. As the stimulator frequency was increased, the finger started to twitch noticeably faster, creating distinct movements from those of the rest of the hand. This was true in both the sensor and optical subsystems. The sensor subsystem, because it was able to detect movement in all three dimensions, was much more sensitive to small changes. The optical subsystem measured only slight changes,



especially as the finger started to curl up more when the stimulation frequency became faster. Fig. 5 demonstrates the frequency component collected that corresponds most heavily to its input stimulation as picked up by the sensor subsystem.

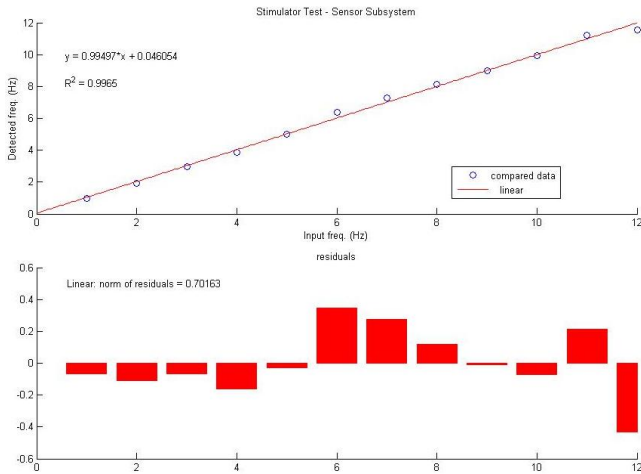


Fig 5. Stimulator Test – Sensor Subsystem

The optical subsystem was testing using induced tremors in the same way as the sensor subsystem. Fig. 6 demonstrates the comparison.

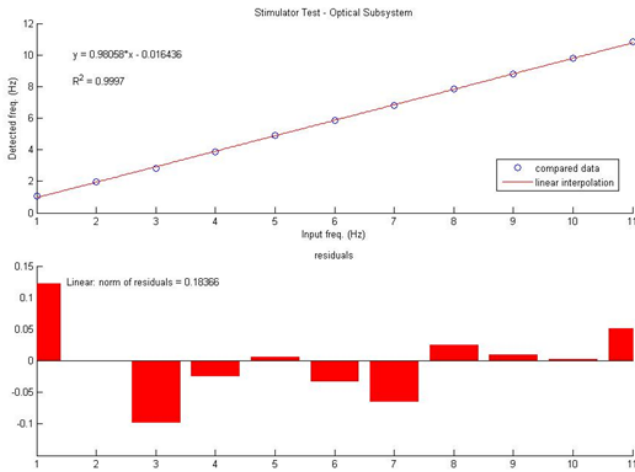


Fig 6. Stimulator Test – Optical Subsystem

Plotting the known frequency with the detected frequency should give a 1:1 relationship in an ideal system. To test this, a linear least squares fitting algorithm was plotted using the data in both instances. Residuals from the least squares fitting are also displayed below each comparison plot. From the algorithm, the sensor subsystem has a linear slope of  $b=0.99497$ . The residuals seem to be the highest towards the middle frequencies, between 6 and 8 Hz. At around 11-12 Hz, detected frequencies started to drift far from the input frequencies. The residuals at this point become very high. This is due to the fact that fatigue occurs at this stage without

increasing the amplitude of the stimulation. Increasing the amplitude, however, hurts the subject. Thus, testing can only be done for a very short period of time. The  $R^2$  value obtained for the sensor subsystem is 0.9965, indicating a good correlation between the detected frequencies and the input ones.

The optical subsystem has a linear slope of  $b=0.9997$ . This demonstrates linearity between the input frequencies and the detected ones, closely giving a 1:1 relationship. This is corresponded by the  $R^2$  value of 0.9997. Thus, the data is linear and well-correlated between the known and the detected values. However, the residuals have values that do not seem to correspond to their frequency positions. This could indicate that the optical system is less dependable than the sensor subsystem.

## V. CONCLUSIONS

The results of the testing of the Clinical Tremor Analysis System demonstrated that while many of the specifications were met, there were some limitations when attempting to test the full range of the system. Due to issues with the testing rig keeping the gears properly attached and aligned at high speeds as well as the inability to fully damp the bounce of the thin board it was difficult to accurately test the system at the high end of the frequency range. In the stimulator test, the high frequencies caused pain and muscle fatigue in the subject limiting testing viability.

For the frequencies that could be tested, both subsystems showed high linearity between the detected frequency and the actual frequency, though there were sometimes high or random residuals. This demonstrates that both subsystems are relatively accurate, with the optical subsystem providing a decent alternative to the sensor subsystem.

This paper has shown that the idea of a cheaper optical system to detect tremors has tremendous potential. In addition, its portability paves the way for new advances in telemedicine for physical therapy. Given the clinical potential of this device, the next step is to test on patients exhibiting real tremors.

## REFERENCES

- [1] Analog Devices Inc, "Digital Accelerometer ADXL345." Last modified 2009. Accessed May 5, 2013. <https://www.sparkfun.com/datasheets/Sensors/Accelerometer/ADXL345.pdf>.
- [2] InvenSense, "IMU 3000IMU-3000 Motion Processing Unit Product Specification ." Last modified 2010. Accessed May 5, 2013. <https://www.sparkfun.com/datasheets/Sensors/IMU/ps-imu-3000a-00-01.1.pdf>.